This is a repository copy of *A method for quantitative analysis of regional lung ventilation using deformable image registration of CT and hybrid hyperpolarized gas/H-1 MRI*.

White Rose Research Online URL for this paper:
http://eprints.whiterose.ac.uk/105957/

Version: Accepted Version

# A method for quantitative analysis of regional lung ventilation using deformable image registration of CT and hybrid hyperpolarised gas/^{1}H MRI

Bilal A. Tahir[1,2], Andrew Swift[2], Helen Marshall[2], Juan Parra-Robles[2], Matthew Q. Hatton[1], Ruth Hartley[3], Richard Kay[4], Christopher E. Brightling[3], Wim Vos[5], Jim M. Wild[2]  and Rob H. Ireland[1,2]

Academic Units of [1]Clinical Oncology and [2]Academic Radiology, University of Sheffield, UK
[3]Institute for Lung Health, University of Leicester, UK
[4]Novartis, Basel, Switzerland
[5]FluidDA nv[2], Kontich, Belgium

**Correspondence**
Rob Ireland, Academic Unit of Clinical Oncology, Weston Park Hospital
University of Sheffield, S10 2SJ, UK
**Email** r.ireland@sheffield.ac.uk

**Short Title**
Hyperpolarised gas MRI and CT image registration

**Abstract**

Hyperpolarized gas MRI generates highly detailed maps of lung ventilation and physiological function while CT provides corresponding anatomical and structural information. Fusion of such complementary images enables quantitative analysis of pulmonary structure-function. However, direct image registration of hyperpolarized gas MRI to CT is problematic, particularly in lungs whose boundaries are difficult to delineate due to ventilation heterogeneity. This study presents a novel indirect method of registering hyperpolarized gas MRI to CT utilizing [1]H-structural MR images that are acquired in the same breath-hold as the gas MRI. The feasibility of using this technique for regional quantification of ventilation of specific pulmonary structures is demonstrated for the lobes.

The direct and indirect methods of hyperpolarized gas MRI to CT image registration were compared using lung images from 15 asthma patients. Both affine and diffeomorphic image transformations were implemented. Registration accuracy was evaluated using the target registration error (TRE) of anatomical landmarks identified on ^{1}H MRI and CT. Wilcoxon signed-rank test was used to test statistical significance.

For the affine transformation, the indirect method of image registration was significantly more accurate than the direct method (TRE=14.7±3.2 vs. 19.6±12.7mm, p=0.036). Using a deformable transformation, the indirect method was also more accurate than the direct method (TRE=13.5±3.3 vs. 20.4±12.8mm, p=0.006).

Accurate image registration is critical for quantification of regional lung ventilation with hyperpolarized gas MRI within the anatomy delineated by CT. Automatic deformable image registration of hyperpolarized gas MRI to CT via same breath-hold ^{1}H MRI is more accurate than direct registration. Potential applications include improved multi-modality image fusion, functionally-weighted radiotherapy planning, and quantification of lobar ventilation in obstructive airways disease.

## 1. Introduction

Computed tomography is the gold standard for high-resolution structural imaging of the lung but has limited functional sensitivity and soft tissue contrast. The quality of proton structural MRI of the lungs has improved in recent years through the use of MR sequences (Wild *et al.*, 2012) such as ultra-short echo time (Lederlin and Crémillieux, 2013) and balanced steady state free precession (Rajaram *et al.*, 2012) to the point where the scans have diagnostic utility in certain conditions. Hyperpolarized gas ($^3$He and $^{129}$Xe) MRI provides highly detailed images of lung ventilation and regional pulmonary function with sensitivity to different aspects of pulmonary physiology and lung disease (Van Beek *et al.*, 2004; Fain *et al.*, 2010). Visualization and quantification of this functional data superimposed upon anatomical images may be advantageous in order to maximize the complementary information relating to form and function.

In practice, fused hyperpolarized gas and anatomical lung imaging could be achieved either by the application of image registration or same breath-hold data acquisition. While hyperpolarized gas and $^1$H MRI is routinely performed in the same imaging session, coil and pulse sequence designs have only recently realized the capability for same breath-hold acquisition of hyperpolarized gas and $^1$H lung MRI (Wild *et al.*, 2011; Wild *et al.*, 2013). Additionally, superior analytical interpretation and quantification is provided by registration of the hyperpolarized gas MRI not only to $^1$H MRI but also to the more detailed images of lung structure provided by high-resolution x-ray CT. However, there is little prospect of a hardware solution for combined MR/CT imaging and as such an image registration solution is required.

Registration of hyperpolarized gas MRI and CT has been shown to facilitate functionally weighted radiotherapy treatment planning for lung cancer patients (Ireland *et al.*, 2007a) and enable comparison of CT and $^3$He MRI measures of ventilation (Mathew *et al.*, 2012). Clinical investigations of other obstructive lung diseases, such as cystic fibrosis, asthma and emphysema (van Beek *et al.*, 2004), could also potentially benefit from the fusion of hyperpolarized gas ventilation MRI with matched anatomical images. In addition, multimodality image fusion of hyperpolarized gas MRI and CT has the potential to facilitate quantification of

ventilation for specific pulmonary structures such as the lobes which cannot be identified on hyperpolarized gas MR images (Tahir *et al.*, 2014).

Preliminary work on hyperpolarized gas MRI to CT image registration demonstrated the feasibility of fusing the images semi-automatically using control point rigid registration (Ireland *et al.*, 2007a). Subsequently, an enhanced acquisition and registration protocol was reported (Ireland *et al.*, 2008). Although hyperpolarized gas MRI to CT registration accuracy was improved, the method still requires the input of operator landmarks that have an associated inter-observer variability. Ideally the registration would be performed fully automatically.

In this study, our first hypothesis is that as the ^{1}H MRI acquired in the same breath-hold as hyperpolarized gas MRI is independent of ventilation defects and structurally similar to the CT then it can facilitate automatic hyperpolarized gas MRI/CT image registration. This is analogous to the way CT images from PET/CT can be used as the intermediary for PET image registration (Ireland *et al.*, 2007b).

A secondary issue with registering hyperpolarized gas MRI to corresponding anatomical images is that quantitative evaluation of registration error is difficult (Ireland *et al.*, 2008), particularly if significant ventilation defects exist. A method that enables calculation of the target registration error (TRE) of corresponding expert defined anatomical landmarks (Murphy *et al.*, 2011) would be beneficial for assessing hyperpolarized gas MRI registration, especially for distinguishing between registration algorithms. Therefore, in this study, our second hypothesis is that inclusion of same breath-hold ^{1}H MRI can provide a method for quantifying the TRE for hyperpolarized gas MR image registration.

In this work, we evaluate the role of synchronously acquired ^{1}H MRI in facilitating automatic hyperpolarized gas MRI/CT image registration and quantitative TRE analysis of hyperpolarized gas MR image registration. In so doing, we demonstrate the feasibility of regional quantification of hyperpolarized gas MR derived ventilation using the underlying lung anatomy from CT.

## 2. Materials and Methods

### 2.1. Image acquisition

The study was performed with national research ethics committee approval. Between February and November 2012, 15 asthma patients gave written informed consent to undergo both hyperpolarized $^3$He MRI and CT during breath hold at functional residual capacity (FRC) + 1L and total lung capacity (TLC), respectively. $^1$H MRI were acquired in the same breath hold as the $^3$He MRI acquisition (Figure 1) (Wild *et al.*, 2011), on a GE HDx 1.5T MR scanner (GE Healthcare, Princeton, NJ, USA). Hyperpolarized $^3$He and $^1$H MR images were acquired with in-plane resolutions of $3 \times 3$ mm$^2$ and $3 \times 6$ mm$^2$ and voxel matrices of $128 \times 128 \times 24$ and $128 \times 64 \times 24$, respectively, and slice thicknesses of 10 mm for both. CT in-plane resolution was approximately $0.86 \times 0.86$ mm$^2$ with a pixel matrix of $512 \times 512$. CT slice thickness was 1 mm with approximately 600 slices for each patient.
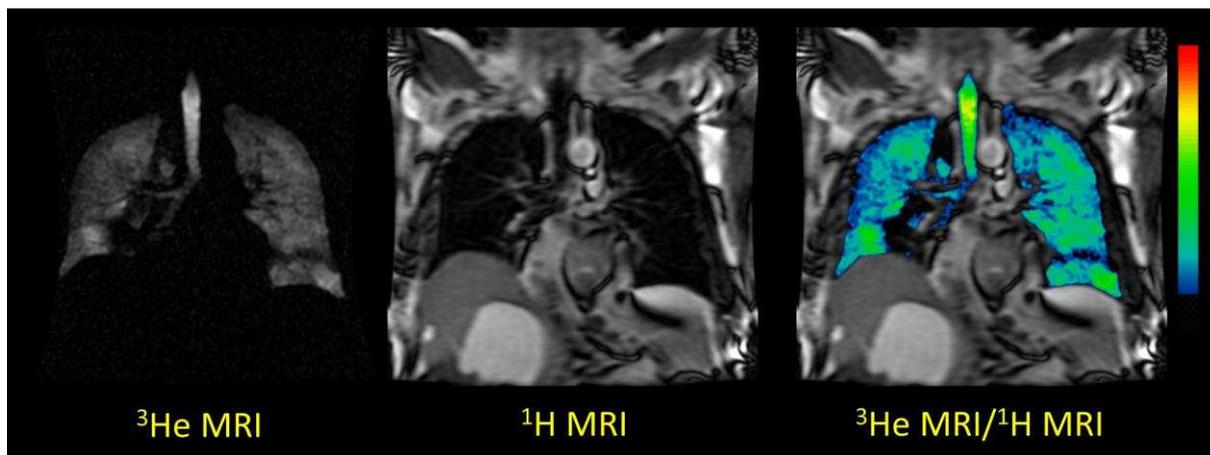


**Figure 1. $^3$He and $^1$H MRI acquired during the same breath-hold for patient 2.**

### 2.2. Image registration

Image registration was performed using the `antsRegistration` tool incorporated as part of the Advanced Normalization Tools (ANTs) (Avants *et al.*, 2011; Avants *et al.*, 2012). For each patient, the $^3$He MRI and $^1$H MRI (moving images) were

registered to CT (fixed image) using affine and diffeomorphic image transformations. CT was resampled to a matrix size of 512 × 512 × 160 voxels to reduce the computational time in performing registrations.

A coarse pre-alignment rigid transform was applied to align the centers of mass of the CT and MR image intensities. The resulting transform was then applied to the affine stage. Due to the multimodal nature of the problem, the mutual information similarity metric was used with 32 histogram bins optimized via the gradient descent algorithm with a step size of 0.1. A multi-resolution Gaussian pyramid with 5 levels was used with down-sampling factors 8x6x4x2x1 and corresponding smoothing Gaussian sigmas of 4x3x2x1x0 mm. A maximum of 10,000 iterations were set for each resolution level to ensure convergence (Glocker *et al.*, 2011).

An additional diffeomorphic transformation that copes with large deformations while preserving topology of anatomical structures (Avants *et al.*, 2008) was also applied to the resulting transform of the affine pipeline with the same parameters for the multi-resolution Gaussian pyramid and similarity metric. The Greedy Symmetric Normalization algorithm (SyN) provided by ANTs registration suite was the chosen diffeomorphic algorithm as it was the highest performing algorithm at a recent pulmonary image registration competition (Murphy *et al.*, 2011). A step size of 0.2 was selected for the gradient descent optimization algorithm.

To reduce the computational time in performing the registration, 16 cores via two Intel Xeon E5-2670 processors @ 2.60 GHz were run in parallel on a 64-bit high performance Linux server (Iceberg, University of Sheffield) using the multi-threading options available in Insight Toolkit version 4 (ITK, www.itk.org). Computational times for the full diffeomorphic pipeline ranged from 28 to 37 minutes, including the rigid pre-alignment and affine stages.

As the $^1$H and $^3$He MRI were acquired in the same breath hold and spatially co-registered (Wild *et al.*, 2011), the same transform to map $^1$H MRI to CT was applied to map $^3$He MRI to CT with linear interpolation for the indirect registrations using the `antsApplyTransform` tool available in ANTs.

## 2.3. Asthma patient study

For each of the fifteen patients, the following four registration pipelines were performed to register $^3$He MRI to CT either directly or indirectly (Figure 2) via the same breath-hold $^1$H MR image:

1. Affine direct             Affine registration of $^3$He MRI to CT
2. Affine indirect           Affine registration of $^1$H MRI to CT
3. Diffeomorphic direct     Diffeomorphic registration of $^3$He MRI to CT
4. Diffeomorphic indirect   Diffeomorphic registration of $^1$H MRI to CT.

For all the registration pipelines, only the transform (affine or diffeomorphic) and moving image ($^3$He MRI for direct and $^1$H MRI for indirect) were varied.
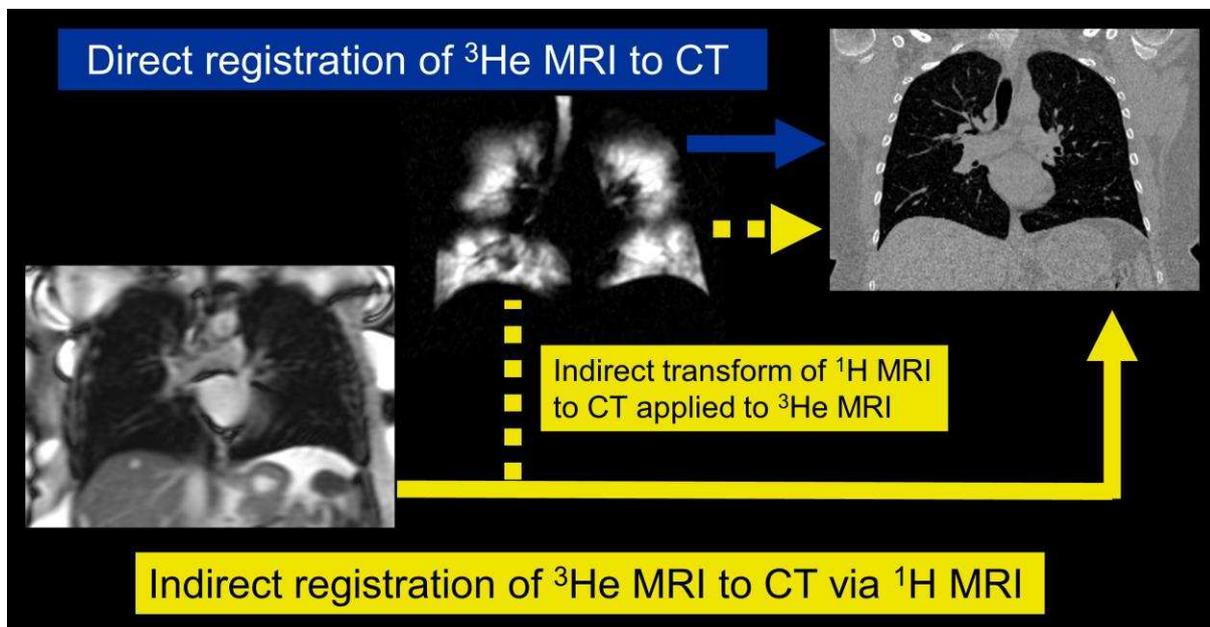


**Figure 2. Workflow of direct and indirect registration methodology.**

## 2.4. Registration evaluation

The registration accuracy of each registration pipeline was assessed quantitatively where pairs of anatomical landmarks were identified by one of the authors (BAT) using Slicer 4 (Fedorov *et al.*, 2012), on the $^1$H MR and CT images and then reviewed independently by a chest radiologist. Landmark locations included the apex and base of the lungs, arch of the aorta and bifurcations of the trachea and blood vessels. The transformations derived from the direct $^3$He MRI to CT and indirect $^1$H MRI to CT registrations were applied to the landmark coordinates to enable the mean target registration error (TRE) of the corresponding landmarks to be calculated for all points. TRE is defined as the Euclidean distance between two corresponding points (Murphy *et al.*, 2011). Figure 3 shows an example of corresponding landmarks identified on $^1$H MRI and CT, alongside the $^3$He MRI that was acquired in the same breath hold as the $^1$H MRI.
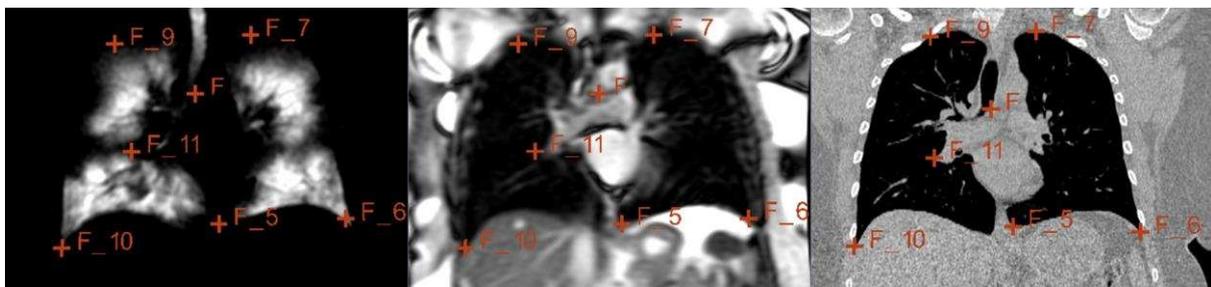


**Figure 3. An example of corresponding landmarks identified on $^1$H MRI (middle) and CT (right) images, alongside the $^3$He MRI (left) that was acquired in the same breath hold as the $^1$H MRI.**

## 2.5. Statistics

The Wilcoxon signed-rank test implemented in IBM SPSS (version 20.0; Chicago, Il, USA) was used to test the statistical significance of the differences between the direct and indirect registration of $^3$He MRI to CT. In addition, the TRE for the indirect diffeomorphic pipeline was compared to all other pipelines. A *p* value less than 0.05 was considered statistically significant.

*2.6. Lobar segmentation and regional ventilation quantification*

As an example to demonstrate the feasibility of quantification of [3]He MRI ventilation of pulmonary structures identifiable only on CT, the percentage ventilation per lobe was calculated by taking the ratio of [3]He MRI volume in a given lobe to the total [3]He MRI volume in the lungs. Medical image segmentation software (Mimics; Materialise, Leuven, Belgium) was used to segment the lobes of CT by identification of fissures in both lungs. These lobar segmentations were used to mask the registered [3]He MRI which were segmented via the Otsu histogram based method which separates the foreground ventilated volume from signal void hypo-ventilated regions and background noise (Otsu, 1979).

## 3. Results

A median of 31 anatomical landmarks per patient (range 22 to 42) were identified on both the ^{1}H MRI and CT images. For this group of patients, the mean±SD target registration error for the direct affine, indirect affine methods, direct diffeomorphic and indirect diffeomorphic algorithms were 19.6±12.7mm, 14.7±3.2mm, 20.4±12.8mm and 13.5±3.3mm, respectively. Table 1 displays the TRE results for all 15 patients. The Wilcoxon signed-rank test demonstrates a statistically significant difference between the direct and indirect affine (p=0.036) and diffeomorphic (p=0.006) methods of image registration. The TRE of 13.5±3.3mm for the diffeomorphic indirect method, using ^{1}H MRI, was more accurate than all the other methods (p values ranging from 0.001 to 0.006).

|  | Affine | | Diffeomorphic | |
| --- | --- | --- | --- | --- |
| Patient | Direct | Indirect | Direct | Indirect |
| 1 | 11.6 | 12.9 | 12.1 | 11.5 |
| 2 | 13.4 | 15.4 | 11.3 | 12.0 |
| 3 | 23.6 | 14.1 | 26.3 | 10.6 |
| 4 | 22.0 | 19.6 | 20.7 | 18.7 |
| 5 | 14.0 | 11.7 | 12.7 | 10.2 |
| 6 | 23.7 | 19.8 | 25.1 | 19.7 |
| 7 | 14.9 | 14.8 | 15.1 | 14.5 |
| 8 | 15.3 | 17.3 | 15.0 | 15.9 |
| 9 | 62.6 | 16.8 | 63.4 | 15.8 |
| 10 | 20.3 | 12.3 | 22.4 | 12.1 |
| 11 | 13.0 | 9.7 | 14.6 | 8.8 |
| 12 | 13.9 | 16.6 | 13.7 | 15.4 |
| 13 | 8.8 | 9.2 | 13.1 | 8.9 |
| 14 | 18.5 | 16.1 | 20.8 | 13.9 |
| 15 | 18.0 | 14.3 | 19.7 | 14.0 |
| Mean | 19.6 | 14.7 | 20.4 | 13.5 |
| SD | 12.7 | 3.2 | 12.8 | 3.3 |
| Median | 15.3 | 14.8 | 15.1 | 13.9 |
| Range | 8.8,62.6 | 9.2,19.8 | 11.3,63.4 | 8.8,19.7 |
| P value Direct vs indirect | 0.036 | | 0.006 | |
| P value vs indirect diffeomorphic | 0.005 | 0.001 | 0.006 | N/A |

**Table 1. Mean target registration errors (in mm) for the direct and indirect affine and diffeomorphic registration methods.**

An example in which the direct method failed was for patient 9, which was characterized by extreme hypoventilation including no ventilation in both the left and right lower lungs (Figure 4). The direct registration broke down for the affine and diffeomorphic methods as the amount of ventilation was insufficient to permit multimodal alignment.
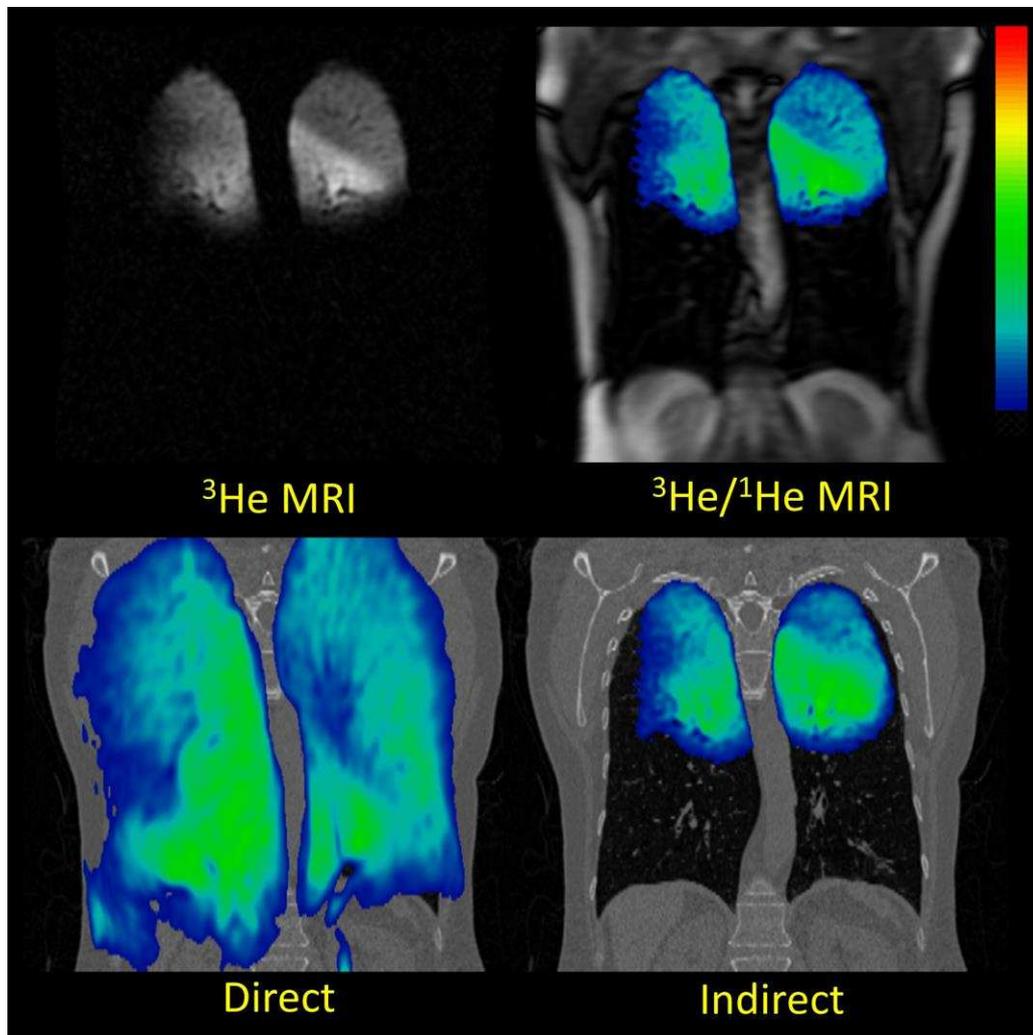


**Figure 4. Corresponding coronal slices of patient 9 showing registered $^{3}$He MRI fused with CT via the direct (bottom left) and indirect (bottom right) diffeomorphic methods with preregistered $^{3}$He MRI (top left) and $^{1}$H MRI fused with $^{3}$He MRI (top right). The direct method breaks down, attempting to stretch the $^{3}$He images which show ventilation in the upper lobes only, across the whole lung.**

Although not as extreme an example, Figure 5 (blue arrow) demonstrates where the direct method inaccurately registers $^{3}$He MRI to CT by increasing the ventilation signal near the base of the left lung. Conversely, the indirect method yields a more clinically realistic registration.
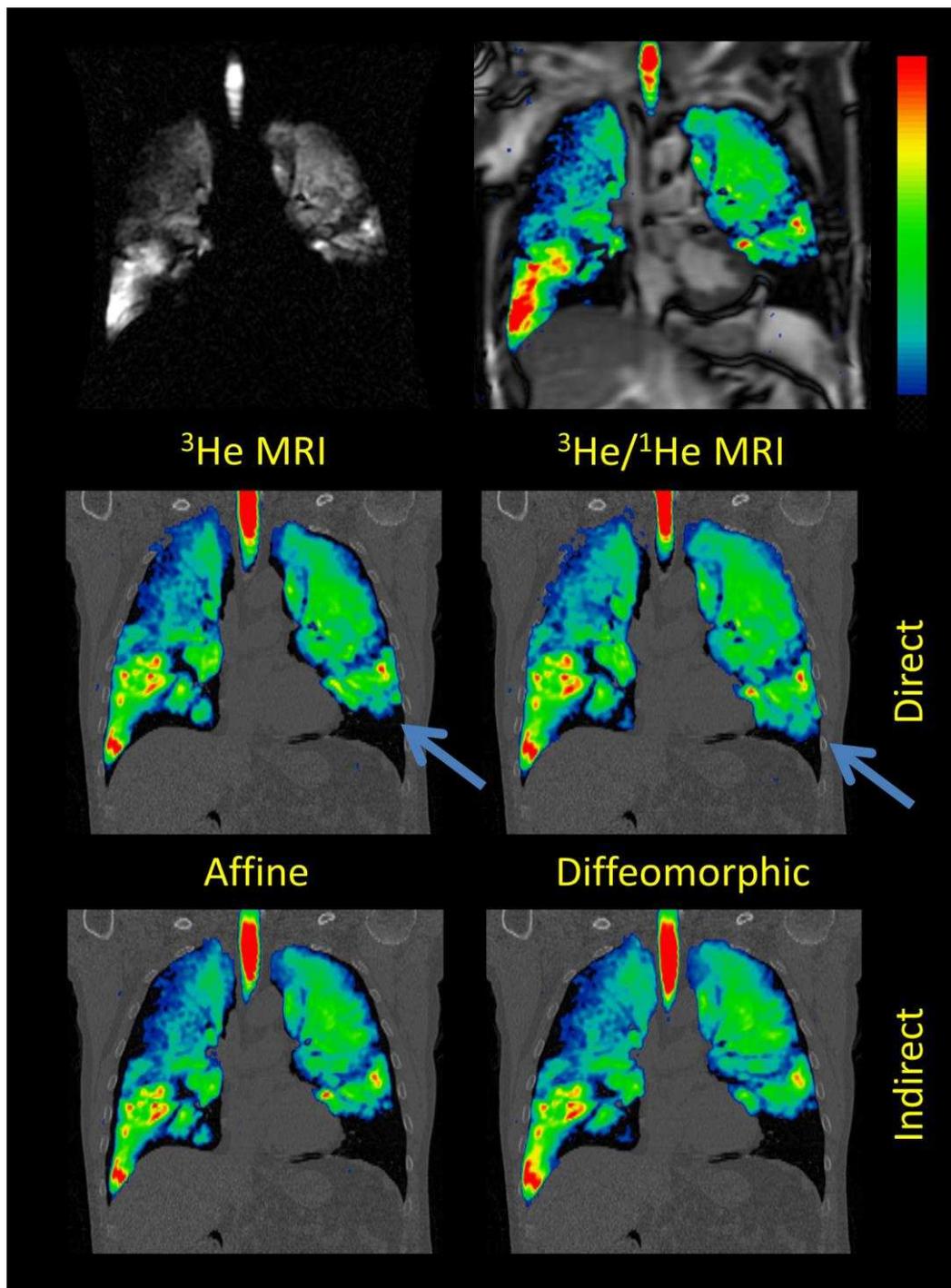
**Figure 5.** Corresponding coronal slices of patient 14 showing registered $^3$He MRI fused with CT via the direct (middle row) and indirect (bottom row) affine and diffeomorphic methods with preregistered $^3$He MRI (top left) and $^1$H MRI fused with $^3$He MRI (top right). The blue arrows near the base of the left lung indicates a registration error in the direct affine and diffeomorphic methods when compared to the corresponding slice of the unregistered $^3$He MRI.

The potential for providing regional quantitative ventilation of specific anatomical structures is demonstrated in Figure 6 for patient 11 where the pulmonary CT lobar masks are superimposed on the registered $^3$He MRI. For this patient, the percentage ventilation for each lobe was RUL=18.39% RML=14.71%, RLL=25.06%, LUL=27.20%, and LLL=14.64%.
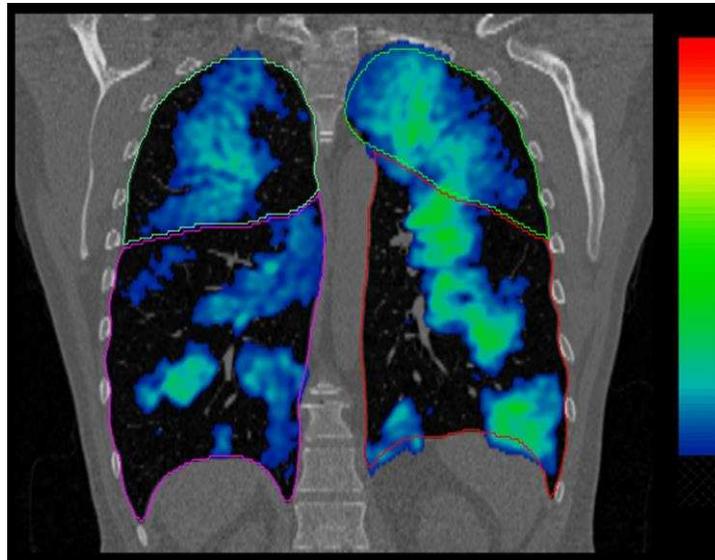


**Figure 6. Example slice of patient 11 showing the CT lobar masks fused with $^3$He MRI after registration.**

## 4. Discussion

Image registration of hyperpolarized gas MRI has previously been published in the context of perfusion MRI using controlled gas administration in pigs (Rizi *et al.*, 2003; Hong *et al.*, 2005) while human *in vivo* $^3$He MRI to CT image registration has been reported as part of a study on the feasibility of lung cancer treatment planning with $^3$He MRI (Ireland *et al.*, 2007a). Furthermore, the importance of the image acquisition procedures on the resultant image registration of $^3$He MRI to CT has been demonstrated (Ireland *et al.*, 2008). When there are major differences in patient positioning and posture between the MRI and CT image acquisitions, there can be large errors in image registration when a rigid algorithm is applied.

The data set used in this study is from asthma patients. A previously reported $^3$He MRI registration paper involved lung cancer patients (Ireland *et al.*, 2008). The

registration accuracy was improved in that work by having the patient positioning match as closely as possible between the MRI and CT acquisitions. In the current work matching MRI and CT patient positioning was not part of the study protocol. The CT was performed in a standard manner, involving a breath hold that was different to that used for the MRI acquisition and with a curved diagnostic bed. The objective of the current study was not to improve upon the radiotherapy level of registration accuracy, but rather to investigate the use of the same breath-hold $^1$H MRI within the image registration and whether it enables target registration error (TRE) analysis to be performed along with quantification of regional ventilation.

In the present work, the additional $^1$H MRI is used as an intermediate step in the registration of hyperpolarized gas MRI to CT. The method of automatic registration assumes intrinsic spatial registration of gas MRI and $^1$H MRI, preferably due to same breath-hold acquisition (Wild *et al.*, 2011), although the method is still potentially viable if hyperpolarized gas and $^1$H MR image registration is required from separate breath-holds (Ireland *et al.*, 2009).

In addition, application of the image registration transformation that is calculated from hyperpolarized gas MRI to CT to the $^1$H MRI landmarks provides a method of assessing the accuracy of gas MRI to CT registration with TRE analysis. Although high quality hyperpolarized gas MR images often contain structural detail that could potentially be used for TRE analysis (Ireland *et al.*, 2008), the advantage of the same breath-hold $^1$H MRI method is that it allows for identification of spatially correlated anatomical landmarks that may not be seen on the hyperpolarized gas MR images due to ventilation defects and partial volume effects.

The indirect affine and diffeomorphic methods demonstrated statistically significant improvements in TRE compared to their corresponding direct methods. The diffeomorphic indirect method of image registration, using $^1$H MRI, was more accurate than the other direct and indirect methods. Due to the differences in breathing maneuver and physiological variations between inter-session CT and MRI scans, the diffeomorphic deformable algorithm was able to account better for large deformations than the affine transformation.

With the direct hyperpolarized gas MRI to CT image registration method, there was no statistically significant improvement in using the diffeomorphic transform. The

direct affine and diffeomorphic registration broke down for one patient in the study (Figure 3) and yielded clinically unrealistic deformations of $^3$He MRI for several patients (Figure 4).

One limitation of our study data is that there is a difference in resolution between the $^1$H MRI and CT images especially in the z direction (10mm vs. 1mm). This may cause observer errors in landmark identification due to partial volume effects at low resolutions. The slice thickness of 10mm was chosen to provide high signal to noise and to ensure full volumetric lung coverage within a breath-hold time achievable by patients, important considerations when both $^3$He and $^1$H images are acquired within the same breath. However, this limitation may be mitigated by recent improvements in MRI technology that provide superior resolution for both same-breath acquired nuclei (Horn *et al.*, 2014).

For this study, only the transform (affine and diffeomorphic) and the moving image ($^3$He MRI for direct and $^1$H MRI for indirect) were varied for each patient while all other registration parameters such as similarity metrics, multiresolution stages and optimization remained constant. Due to inter-patient variations in ventilation heterogeneity and respiratory states, further improvements in registration may be gained by patient specific parameterization.

There are many potential clinical applications of improved hyperpolarized gas MR image registration since accurate registration of anatomical and functional images can enhance both image interpretation and quantification. For a variety of lung diseases, registration of hyperpolarized gas MRI to CT would enable the pulmonary ventilation to be assessed against the underlying anatomical CT structure, which serves as the gold standard. The feasibility of using the indirect registration technique for regional quantification of ventilation of specific pulmonary structures is demonstrated in Figure 6. In addition, registration to CT is critical in radiotherapy for the implementation of functionally weighted treatment planning (Ireland *et al.*, 2007a; Bates *et al.*, 2009; Partridge *et al.*, 2010).

## 5. Conclusion

This study demonstrates the benefit of a method of automatic image registration of hyperpolarized gas MRI to CT indirectly via a $^1$H MRI that is acquired in the same

breath-hold as gas MRI data. This study also shows that inclusion of same breath-hold ^{1}H MRI enables TRE quantification of hyperpolarized gas MRI to CT image registration. Evaluation in 15 clinical cases demonstrates that TRE analysis is practical and that image registration accuracy can be improved when the additional anatomical ^{1}H MRI information is incorporated. Accurate image registration is critical for quantification of regional ventilation using hyperpolarized gas MRI and CT.

## Acknowledgements

## References

Avants B, Tustison N, Song G, Wu B, Stauffer M, McCormick M, Johnson H and Gee J 2012 A unified image registration framework for ITK *Lect. Notes Comput. Sc.* **7359** 266-75

Avants B B, Epstein C L, Grossman M and Gee J C 2008 Symmetric diffeomorphic image registration with cross-correlation: evaluating automated labeling of elderly and neurodegenerative brain *Med. Image Anal.* **12** 26-41

Avants B B, Tustison N J, Song G, Cook P A, Klein A and Gee J C 2011 A reproducible evaluation of ANTs similarity metric performance in brain image registration *NeuroImage* **54** 2033-44

Bates E L, Bragg C M, Wild J M, Hatton M Q and Ireland R H 2009 Functional image-based radiotherapy planning for non-small cell lung cancer: A simulation study *Radiother. Oncol.* **93** 32-6

Fain S, Schiebler M L, McCormack D G and Parraga G 2010 Imaging of lung function using hyperpolarized helium-3 magnetic resonance imaging: Review of current and emerging translational methods and applications *Magn. Reson. Imag.* **32** 1398-1408

Fedorov A, Beichel R, Kalpathy-Cramer J, Finet J, Fillion-Robin J, Pujol S, Bauer C, Jennings D, Fennessy F, Sonka M, Buatti J, Aylward S, Miller J, Pieper S and Kikinis R 2012 3D Slicer as an image computing platform for the Quantitative Imaging Network *Magn. Reson. Imaging* **30** 1323-41

Glocker B, Sotiras A, Komodakis N and Paragios N 2011 Deformable medical image registration: setting the state of the art with discrete methods *Annu. Rev. Biomed. Eng.* **13** 219-44

Hong C, Leawoods J C, Yablonskiy D A, Leyendecker J R, Bae K T, Pilgram T K, Woodard P K, Conradi M S and Zheng J 2005 Feasibility of combining MR perfusion, angiography, and 3He ventilation imaging for evaluation of lung function in a porcine model *Acad. Radiol.* **12** 202-9

Horn F C, Tahir B A, Stewart N J, Collier G J, Norquay G, Leung G, Ireland R H, Parra-Robles J, Marshall H, Wild J M 2014 Lung ventilation volumetry with same-breath acquisition of hyperpolarized gas and proton MRI *NMR Biomed.* doi: 10.1002/nbm.3187. [Epub ahead of print]

Ireland R H, Woodhouse N, Swinscoe J A, Hatton M Q and Wild J M 2009 Towards automatic image registration of hyperpolarized 3He MRI and x-ray CT images of the lung *Proc. Intl. Soc. Mag. Reson. Med.* **17** 2197

Ireland R H, Bragg C M, McJury M, Woodhouse N, Fichele S, van Beek E J, Wild J M and Hatton M Q 2007a Feasibility of image registration and intensity-modulated radiotherapy planning with hyperpolarized helium-3 magnetic resonance imaging for non-small-cell lung cancer *Int. J. Radiat. Oncol. Biol. Phys.* **68** 273-81

Ireland R H, Dyker K E, Barber D C, Wood S M, Hanney M B, Tindale W B, Woodhouse N, Hoggard N, Conway J and Robinson M H 2007b Nonrigid image registration for head and neck cancer radiotherapy treatment planning with PET/CT *Int. J. Radiat. Oncol. Biol. Phys.* **68** 952-7

Ireland R H, Woodhouse N, Hoggard N, Swinscoe J A, Foran B H, Hatton M Q and Wild J M 2008 An image acquisition and registration strategy for the fusion of hyperpolarized helium-3 MRI and x-ray CT images of the lung *Phys. Med. Biol.* **53** 6055-63

Lederlin M and Crémillieux Y 2013 Three-dimensional assessment of lung tissue density using a clinical ultrashort echo time at 3 tesla: A feasibility study in healthy subjects *J. Magn. Reson. Imaging* doi: 10.1002/jmri.24429

Mathew L, Wheatley A, Castillo R, Castillo E, Rodrigues G, Guerrero T and Parraga G 2012 Hyperpolarized (3)He magnetic resonance imaging: comparison with four-dimensional x-ray computed tomography imaging in lung cancer *Acad. Radiol.* **19** 1546-53

Murphy K, van Ginneken B, Reinhardt J M, Kabus S, Ding K, Deng X, Cao K, Du K, Christensen G E, Garcia V, Vercauteren T, Ayache N, Commowick O, Malandain G, Glocker B, Paragios N, Navab N, Gorbunova V, Sporring J, de Bruijne M, Han X, Heinrich M P, Schnabel J A, Jenkinson M, Lorenz C, Modat M, McClelland J R, Ourselin S, Muenzing S E, Viergever M A, De Nigris D, Collins D L, Arbel T, Peroni M, Li R, Sharp G C, Schmidt-Richberg A, Ehrhardt J, Werner R, Smeets D, Loeckx D, Song G, Tustison N, Avants B, Gee J C, Staring M, Klein S, Stoel B C, Urschler M, Werlberger M, Vandemeulebroucke J, Rit S, Sarrut D and Pluim J P 2011 Evaluation of registration methods on thoracic CT: the EMPIRE10 challenge *IEEE Trans. Med. Imaging* **30** 1901-20

Otsu N 1979 A threshold selection method from gray-level histograms *IEEE Trans. Syst. Man Cybern.* **9** 62-6

Partridge M, Yamamoto T, Grau C, Hoyer M and Muren L P 2010 Imaging of normal lung, liver and parotid gland function for radiotherapy *Acta Oncol.* **49** 997-1011

Rajaram S, Swift A J, Capener D, Telfer A, Davies C, Hill C, Condliffe R, Elliot C, Hurdman J, Kiely D G and Wild J M 2012 Lung morphology assessment with balanced steady-state free precession MR imaging compared with CT *Radiology* **263** 569-77

Rizi R R, Saha P K, Wang B, Ferrante M A, Lipson D, Baumgardner J and Roberts D A 2003 Co-registration of acquired MR ventilation and perfusion images--validation in a porcine model *Magn. Reson. Med.* **49** 13-8

Tahir B A, Holsbeke C V, Ireland R H, Swift A J, Marshall H, Parra-Robles J, Hartley R, Laurencin M, Kay R, Siddiqui S, Brightling C E, Backer J D, Vos W and Wild J M 2014 Comparison of CT-based lobar ventilation models with helium-3 MRI ventilation measurements in asthmatics *Am. J. Respir. Crit. Care Med.* **189** A2391

van Beek E J, Wild J M, Kauczor H U, Schreiber W, Mugler J P, 3rd and de Lange E E 2004 Functional MRI of the lung using hyperpolarized 3-helium gas *J. Magn. Reson. Imaging* **20** 540-54

Wild J M, Ajraoui S, Deppe M H, Parnell S R, Marshall H, Parra-Robles J and Ireland R H 2011 Synchronous acquisition of hyperpolarised 3He and 1H MR images of the lungs - maximising mutual anatomical and functional information *NMR Biomed.* **24** 130-4

Wild J M, Marshall H, Bock M, Schad L R, Jakob P M, Puderbach M, Molinari F, Van Beek E J R and Biederer J 2012 MRI of the lung (1/3): methods *Insights Imaging* **3** 345-53

Wild J M, Marshall H, Xu X, Norquay G, Parnell S R, Clemence M, Griffiths P D and Parra-Robles J 2013 Simultaneous imaging of lung structure and function with triple-nuclear hybrid MR imaging *Radiology* **267** 251-5